Tunable Optoelectronic Oscillator Based on a Polarization Modulator and a Chirped FBG

Zhenzhou Tang, Shilong Pan, *Member, IEEE*, Dan Zhu, Ronghui Guo, Yongjiu Zhao, Minghai Pan, De Ben, and Jianping Yao, *Fellow, IEEE*

***Abstract*— A wideband-tunable optoelectronic oscillator (OEO) is proposed and experimentally demonstrated based on a tunable microwave photonic filter (MPF) consisting of a polarization modulator, a chirped fiber Bragg grating, and a polarization beam splitter (PBS). By simply adjusting the polarization state of the signal before the PBS, the center frequency of the MPF is tuned. The proposed OEO is experimentally demonstrated. A high-purity microwave signal with a tunable frequency within 5.8–11.8 GHz is generated. The single-sideband phase noise of the generated signal is −104.56 dBc/Hz at 10-kHz offset.**

***Index Terms*— Microwave generation, microwave photonics, optoelectronic oscillator (OEO), polarization modulation.**

I. Introduction

OPTOELECTRONIC oscillators (OEO) have attracted great interests for possible applications in radars, communications, and modern instrumentation thanks to their inherent capability to generate microwave or millimeter-wave signals with ultra-low phase noise [1]. Most of the OEOs proposed in the past, however, have a small frequency tuning range due to the poor tunability of a high-Q microwave bandpass filter (BPF) in an OEO loop for mode selection [2]. Although some microwave filters, such as a Yttrium-iron-garnet (YIG) BPF, can have a tunable range in the GHz range [3], a highly stable drive current source has to be used, which is usually bulky and costly. To overcome the problem, several approaches to tune the OEO in the optical domain were reported [4]–[9]. In [6], we proposed an OEO tunable from 6.41 to 10.85 GHz based on a Fabry-Perot laser diode (LD). However, the stability of the OEO is poor since the wavelength drift of the LD will directly affect the frequency of the OEO. A joint operation of a phase modulator and a dispersive element would produce a tunable microwave photonic bandpass filter (MPF), which has been used to implement a tunable OEO [7], but the frequency tuning is also achieved by tuning the wavelength of the laser source. Recently, a frequency tunable OEO was reported by phase modulation or single-sideband modulation followed by a narrowband phase-shifted fiber Bragg grating (FBG) [8], [9], but again the frequency of the oscillation signal is sensitive to the wavelength drift of the laser source.

In this letter, we propose and demonstrate a novel tunable OEO based on a microwave photonic filter consisting of a polarization modulator (PolM) and a chirped FBG (CFBG). The CFBG serves as a dispersive element. The PolM together with a polarization beam splitter (PBS) performs simultaneously amplitude modulation and phase modulation, with the ratio between the two modulations adjusted by changing the polarization state of the optical signal between the PolM and the PBS. Since the transmission response of an amplitude-modulated signal decreases with frequency and that of a phase-modulated signal increases with frequency in a dispersive element, the change of the ratio between the two modulations would lead to a shift of the transmission response of the entire signal [10]. A tunable MPF for a coarse selection of the oscillation mode in the OEO is thus formed. In addition, the PBS is used to form dual loops. Fine selection of the oscillation mode is achieved by the Vernier effect.

II. Principle

Fig. 1 shows the schematic of the proposed tunable OEO. The key component in the OEO is the tunable MPF formed by a PolM, a CFBG, two polarization controllers (PCs) and a PBS. When a light wave that is aligned via a PC (PC1) at an angle of 45° to one principal axis of the PolM is coupled into the PolM, two phase-modulated optical waves along the two principal axes are generated [11]

$$\begin{bmatrix} E_x \\ E_y \end{bmatrix} = \frac{\sqrt{2}}{2}\begin{bmatrix} [jJ_1(\gamma)e^{-j\omega_m t} + J_0(\gamma) + jJ_1(\gamma)e^{j\omega_m t}] \\ [-jJ_1(\gamma)e^{-j\omega_m t} + J_0(\gamma) - jJ_1(\gamma)e^{j\omega_m t}] \end{bmatrix} \tag{1}$$

where ω_c is the angular frequency of the optical carrier, γ is the modulation index, ω_m is the angular frequency of the generated signal, $J_n(\gamma)$ is the nth-order Bessel function of the first kind. In (1), higher-order (≥ 2) terms are ignored due to a

Manuscript received April 4, 2012; revised June 9, 2012; accepted June 12, 2012. Date of publication June 12, 2012; date of current version July 31, 2012. This work was supported in part by the Ph.D. Programs Foundation of the Ministry of Education of China under Grant 20113218120018, the Program for New Century Excellent Talents in University under Grant NCET-10-0072, the National Basic Research Program of China under Grant 2012CB315705, the National Natural Science Foundation of China under Grant 61107063, and the Fok Ying Tung Education Foundation.

Z. Tang, S. Pan, D. Zhu, R. Guo, Y. Zhao, M. Pan, and D. Ben are with the Microwave Photonics Research Laboratory, College of Electronic and Information Engineering, Nanjing University of Aeronautics and Astronautics, Nanjing 210016, China. They are also with the State Key Laboratory of Millimeter Waves, Nanjing 210096, China (e-mail: pans@ieee.org).

J. Yao is with the Microwave Photonics Research Laboratory, College of Electronic and Information Engineering, Nanjing University of Aeronautics and Astronautics, Nanjing 210016, China, and also with the Microwave Photonics Research Laboratory, School of Electrical Engineering and Computer Science, University of Ottawa, Ottawa, ON K1N 6N5, Canada.

Color versions of one or more of the figures in this letter are available online at http://ieeexplore.ieee.org.

Digital Object Identifier 10.1109/LPT.2012.2205235

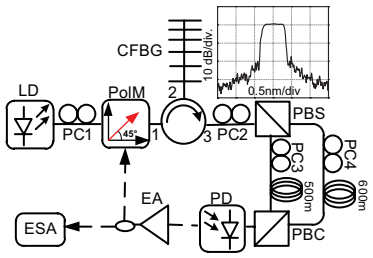

Fig. 1. Schematic diagram of the proposed tunable optoelectronic oscillator. Insert: reflection response of the CFBG. LD: laser diode. PC: polarization controller. PolM: polarization modulator. PBS: polarization beam splitter. PBC: polarization beam combiner. EA: electrical amplifier. PD: photodetector. CFBG: chirped fiber Bragg grating. ESA: electrical spectrum analyzer.

small-signal modulation. The modulated signal is sent to the CFBG via an optical circulator, which functions as a dispersive element. The reflected signal is given by

$$\begin{bmatrix} E_x \\ E_y \end{bmatrix} \propto \frac{\sqrt{2}}{2} \begin{bmatrix} \left[j J_1(\gamma) e^{-j\left(\omega_m t - \theta_{-1}\right)} \right. \\ \left. + J_0(\gamma) e^{j\theta_0} + j J_1(\gamma) e^{j\left(\omega_m t + \theta_1\right)} \right] \\ \left[- j J_1(\gamma) e^{-j\left(\omega_m t - \theta_{-1}\right)} \right. \\ \left. + J_0(\gamma) e^{j\theta_0} - j J_1(\gamma) e^{j\left(\omega_m t + \theta_1\right)} \right] \end{bmatrix} \quad (2)$$

where $\theta_0 = z\beta(\omega_c)$, $\theta_1 = z\beta(\omega_c) + \tau_0\omega_m + 1/2 D_\omega \omega_m^2$, and $\theta_{-1} = z\beta(\omega_c) - \tau_0\omega_m + 1/2 D_\omega \omega_m^2$ are the dispersion-induced phase shifts to the optical carrier and the upper and lower sidebands, respectively, where z is the traveled distance, $\beta(\omega_c)$ is the propagation constant at ω_c, $\tau_0 = z\beta'(\omega_c)$ and $D_\omega = z\beta''(\omega_c)$. E_x and E_y are then combined by a PBS whose principal axis is oriented at an angle of α to one principal axis of the PolM, we obtain

$$\begin{aligned} E(t) &= \cos\alpha E_x e^{j\phi_0} + \sin\alpha E_y \\ &\propto J_0(\gamma)\left(e^{j(\theta_0+\phi_0)}\cos\alpha + e^{j\theta_0}\sin\alpha\right) \\ &+ j J_1(\gamma)\cos\alpha\left(e^{j(-\omega_m t+\phi_0+\theta_{-1})} + e^{j(\omega_m t+\phi_0+\theta_{+1})}\right) \\ &- j J_1(\gamma)\sin\alpha\left(e^{j(-\omega_m t+\theta_{-1})} + e^{j(\omega_m t+\theta_{+1})}\right) \end{aligned} \quad (3)$$

where φ_0 is the phase difference between E_x and E_y which can be adjusted by tuning the DC bias applied to the PolM. polmhe signal at the output of the PBS is sent to a photodetector (PD), and let φ_0 be $\pi/2$, the AC term of the detected signal is given by

$$\begin{aligned} i_{AC} \propto |E(t)|^2 &= 2J_0(\gamma) J_1(\gamma) \\ &\times \sin\left(2\alpha + \frac{1}{2} D_\omega \omega_m^2\right) \cos[\omega_m (t - \tau_0)] \end{aligned} \quad (4)$$

As can be seen, the generated electrical signal has a coefficient given by $\eta = \sin(2\alpha + 1/2 D_\omega \omega_m^2)$, so the power varies as a function of the angular frequency ω_m. Obviously, if $2\alpha + 1/2 D_\omega \omega_m^2 = (2k+1)\pi/2$, k = 0, ±1, ±2..., the signal at ω_m will have a maximum transmittance. That is to say, the frequency of the transmission peak is

$$\omega_m = \sqrt{((2k+1)\pi - 4\alpha)/D_\omega} \, (k = 0, \pm 1, \pm 2...) \quad (5)$$

Since α can be tuned by PC2, the peak of the transmission response can be shifted to any desired frequency.

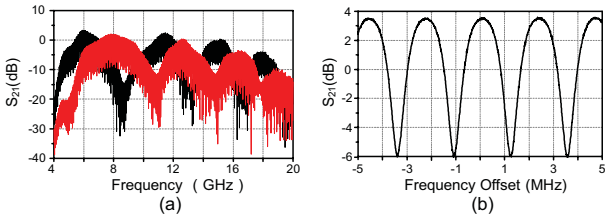

Fig. 2. (a) Open-loop responses of the OEO at two typical settings of PC2. (b) Zoom-in view of the transmission peak at 6 GHz.

A wavelength-independent and frequency-tunable MPF is thus realized.

It should be noted that the length of an OEO loop usually ranges from several meters to tens of kilometers, which makes the OEO to have densely spaced oscillation modes. The 3-dB bandwidth of the MPF based on the PolM and the CFBG is not narrow enough to guarantee a single-frequency oscillation. Therefore, the PBS is also used as a power divider to form two paths. Each path has a section of single-mode fiber (SMF) and a PC. The two paths are combined by a polarization beam combiner (PBC). Two polarization-multiplexed loops are thus formed in the OEO [12]. With the coarse mode selection by the MPF and the fine mode selection by the dual loops, a tunable OEO with high side-mode suppression is obtained.

III. Experiment Results and Discussions

An experiment based on the configuration in Fig. 1 is carried out. A light wave is generated by a tunable laser source (Agilent N7714A) and is sent to the PolM via PC1. The PolM (Versawave Inc) has a 3-dB bandwidth of 40 GHz and a half-wave voltage of 3.5 V. The lengths of the SMF in the dual loops are ~500 and ~600 m. The PD has a bandwidth of 40 GHz and a responsivity of 0.65 A/W. The gain of the electrical amplifier (EA) in the experiment is about 40 dB with a bandwidth of 5.8-20 GHz. The reflection response of the CFBG is shown as the inset of Fig. 1, which has a 3-dB bandwidth of 0.6 nm with a center wavelength of 1557.54 nm and a dispersion of −1445 ps/nm. An electrical spectrum analyzer (Agilent E4447AU) is connected to the EA to observe the electrical spectrum of the generated microwave signal and to measure its phase noise.

Fig. 2 shows the open-loop responses of the OEO measured by a vector network analyzer. As can be seen from Fig. 2(a), the peak of the open-loop response is shifted from 6 GHz to 7.8 GHz by simply adjusting PC2. The profile of the open-loop response is mainly determined by the dispersion-induced MPF, which has a 3-dB passband of about 2 GHz around the highest peak. Fig. 2(b) shows the zoom-in view of the transmission peak at 6 GHz. As can be seen, the free spectral range (FSR) of the comb filter formed by the dual loops is about 2.3 MHz, which is determined by the length difference of the two paths, i.e. about 100 m.

By closing the loop, the OEO starts to oscillate at the frequency around the transmission peak of the MPF. The vernier effect formed by the dual loops would perform the fine mode selection of the OEO. Fig. 3(a) shows a typical electrical spectrum of an oscillating signal, which has a frequency

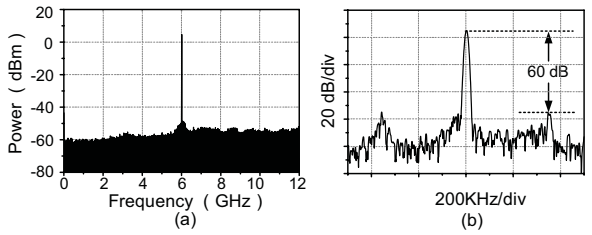

Fig. 3. (a) Electrical spectrum of the 6-GHz microwave signal. (b) Zoom-in view of the 6 GHz signal at a span of 1 MHz.

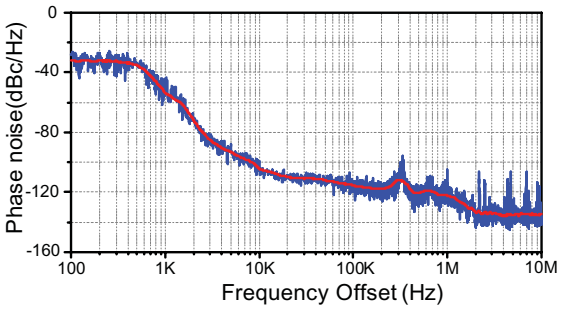

Fig. 4. Phase noise spectrum of the generated 6-GHz signal.

of 6 GHz. The zoom-in view of the 6-GHz microwave signal is shown in Fig. 3(b). The side mode suppression ratio is greater than 60 dB. The single-sideband (SSB) phase noise of the oscillating signal is also measured. As can be seen in Fig. 4, the phase noise of the 6-GHz microwave signal is −104.56 dBc/Hz at 10-KHz offset. The sidemodes have a maximal phase noise of −95 dBc/Hz, indicating that the spectral purity of the OEO is high. It should be noted that the phase noise measurement based on the electrical spectrum analyzer would be affected by the intensity noise, so the actual performance should be better than the measured cases.

The stability of the oscillating signal is also evaluated. During more than half an hour observation, no mode hopping is found. Since the OEO is operated at a laboratory environment and no mechanical, thermal and acoustic isolation or phase locking loop is used, the frequency drift of the oscillation signal is about 100 kHz.

By adjusting PC2, the frequency of the oscillating signal can be tuned in a wide range. Fig. 5 shows the electrical spectra of the generated signal over a frequency ranging from 5.8 to 11.8 GHz with a tuning step of 100 MHz. The operational frequency of the OEO is restricted by the frequency response of the electrical or electro-optical devices and the dispersion parameter of the CFBG. Note that some frequencies can not be achieved due to the uneven frequency response of the electrical or the electro-optical devices in the system. For instance, the EA used in the experiment has a small notch around 10 GHz, so we can only observe oscillation signal at a higher frequency, corresponding to the second peak of the MPF. If the gain of the OEO is flattened, the frequency tuning range covering 5.8 to 11.8 GHz would be achievable, and a constant output power would also be maintained.

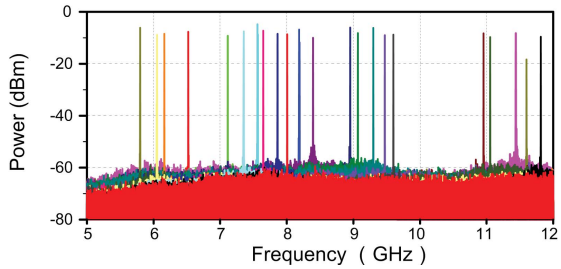

Fig. 5. Measured electrical spectra of the generated microwave signal at different PC2 settings.

IV. Conclusion

We have proposed and demonstrated a tunable OEO based on a MPF. The PolM and the CFBG, in conjunction with a PBS, was operating as an optically tunable MPF, which was employed to perform coarse frequency tuning. The fine frequency tuning was achieved by the dual-loop configuration. The proposed OEO was experimentally demonstrated. A tunable microwave signal within 5.8 to 11.8 GHz was achieved. The SSB phase noise of the generated signal was also measured, which was −104.56 dBc/Hz at 10-kHz offset.

References

[1] X. S. Yao and L. Maleki, "Optoelectronic oscillator for photonic systems," *IEEE J. Quantum Electron.*, vol. 32, no. 7, pp. 1141–1149, Jul. 1996.

[2] S. Poinsot, H. Porte, J. Goedgebuer, W. T. Rhodes, and B. Boussert, "Continuous radio-frequency tuning of an optoelectronic oscillator with dispersive feedback," *Opt. Lett.*, vol. 27, no. 15, pp. 1300–1302, Aug. 2002.

[3] D. Zhu, S. L. Pan, and D. Ben, "Tunable frequency-quadrupling dual-loop optoelectronic oscillator," *IEEE Photon. Technol. Lett.*, vol. 24, no. 3, pp. 194–196, Feb. 1, 2012.

[4] S. Fedderwitz, A. Stohr, S. Babiel, V. Rymanov, and D. Jager, "Opto-electronic K-band oscillator with gigahertz tuning range and low phase noise," *IEEE Photon. Technol. Lett.*, vol. 22, no. 20, pp. 1497–1499, Oct. 15, 2010.

[5] I. Ozdur, D. Mandridis, N. Hoghooghi, and P. J. Delfyett, "Low noise optically tunable opto-electronic oscillator with Fabry–Pérot etalon," *J. Lightw. Technol.*, vol. 28, no. 21, pp. 3100–3106, Nov. 1, 2010.

[6] S. Pan and J. Yao, "Wideband and frequency-tunable microwave generation using an optoelectronic oscillator incorporating a Fabry–Pérot laser diode with external optical injection," *Opt. Lett.*, vol. 35, pp. 1911–1913, Jun. 2010.

[7] W. Li and J. P. Yao, "An optically tunable optoelectronic oscillator," *J. Lightw. Technol.*, vol. 28, no. 18, pp. 2640–2645, Sep. 15, 2010.

[8] W. Li and J. P. Yao, "An optically tunable frequency-doubling optoelectronic oscillator incorporating a phase-shifted-fiber-Bragg-grating based frequency-tunable photonic microwave filter," in *Proc. MWP/APMP 2011*, Oct., pp. 429–432.

[9] B. Yang, X. F. Jin, X. M. Zhang, S. L. Zheng, H. Chi, and Y. Wang, "A wideband frequency-tunable optoelectronic oscillator based on a narrowband phase-shifted FBG and wavelength tuning of laser," *IEEE Photon. Technol. Lett.*, vol. 24, no. 1, pp. 73–75, Jan. 1, 2012.

[10] H. T. Zhang, S. L. Pan, M. H. Huang, and X. F. Chen, "A polarization-modulated analog photonic link with compensation of the dispersion-induced power fading," *Opt. Lett.*, vol. 37, no. 5, pp. 866–868, Mar. 2012.

[11] S. L. Pan and J. P. Yao, "A frequency-doubling optoelectronic oscillator using a polarization modulator," *IEEE Photon. Technol. Lett.*, vol. 21, no. 13, pp. 929–931, Jul. 1, 2009.

[12] S. H. Cai, S. L. Pan, D. Zhu, Z. Z. Tang, P. Zhou, and X. F. Chen, "Coupled frequency-doubling optoelectronic oscillator based on polarization modulation and polarization multiplexing," *Opt. Commun.*, vol. 285, no. 6, pp. 1140–1143, Mar. 2012.